Orbital character of states at the Fermi level in $La_{2-x}Sr_xCuO_4$ and $R_{2-x}Ce_xCuO_4$ (R =Nd,Sm)

E. Pellegrin, N. Nücker, and J. Fink
Kernforschungszentrum Karlsruhe, Institut für Nukleare Festkörperphysik, Postfach 3640, W-7500 Karlsruhe, Germany

S. L. Molodtsov, A. Gutiérrez, E. Navas, O. Strebel, Z. Hu, M. Domke, and G. Kaindl
Institut für Experimentalphysik, Freie Universität Berlin, Arnimallee 14, W-1000 Berlin 33, Germany

S. Uchida and Y. Nakamura
Department of Applied Physics, University of Tokyo, Bunkyo-Ku, Tokyo 113, Japan

J. Markl, M. Klauda, and G. Saemann-Ischenko
Physikalisches Institut der Universität Erlangen, W-8520 Erlangen, Germany

A. Krol
Department of Physics, State University of New York (SUNY), Buffalo, New York 14260

J. L. Peng, Z. Y. Li, and R. L. Greene
Center for Superconductivity Research, Department of Physics, University of Maryland, College Park, Maryland 20742
(Received 10 August 1992; revised manuscript received 19 October 1992)

Polarization-dependent x-ray-absorption spectroscopy on the O 1s and Cu 2p edges using the non-surface-sensitive fluorescence method has been performed on single crystals of $La_{2-x}Sr_xCuO_{4+\delta}$, $R_{2-x}Ce_xCuO_{4-\delta}$ (R =Nd and Sm), and the insulating compound $Ca_{0.86}Sr_{0.14}CuO_2$. The experimental results support the picture of a doped charge-transfer insulator. The symmetry of hole states on O and Cu sites has been determined. These have predominantly in-plane, i.e., O $2p_{x,y}$ and Cu $3d_{x^2-y^2}$ character. In p-type doped cuprates for $0<x<0.15$ about 8% of the total number of hole states on O sites have O $2p_z$ character, which probably originates from apical O sites. At higher dopant concentration, this number increases. In the n-type doped system 4–11 % of the O 2p states in the energy range of the upper Hubbard band have O $2p_z$ character. In nearly all the systems investigated in this work the fraction of unoccupied Cu $3d_{3z^2-r^2}$ states with respect to the total number of Cu holes in the upper Hubbard band is 3±3 %. At higher energies a high spectral weight with Cu $3d_{3z^2-r^2}$ character (about 40% of the total amount of unoccupied Cu 3d states in the upper Hubbard band) is observed, which is probably caused by a hybridization with Cu 4s and 4p states. The implication of holes in nonplanar orbitals on high-T_c superconductivity in cuprates is discussed.

I. INTRODUCTION

It is generally believed that the CuO_2 planes are the essential ones for superconductivity in cuprate superconductors. Due to strong on-site correlations on the Cu sites, the electronic structure of these CuO_2 planes is difficult to describe theoretically. Therefore, approximations are introduced. Very often, among the many orbitals which may be important for the electronic structure of cuprates, only Cu $3d_{x^2-y^2}$ and O $2p_{x,y}$ orbitals, which point towards the Cu atoms (O $2p_\sigma$) are taken into account. This leads to the three-band Hubbard model introduced by Emery[1] and by Varma, Schmitt-Rink, and Abrahams.[2]

The parameters of the model Hamiltonian, as derived from experiments or from local-density approximation (LDA) band-structure calculations, indicate that the undoped parent compounds such as La_2CuO_4 or Nd_2CuO_4 can be viewed as charge-transfer insulators in the classification scheme of Zaanen, Sawatzky, and Allen.[3] The high-T_c superconductors are then reached by p- or n-type doping, leading to holes in the valence band with predominantly O 2p character or electrons in the conduction band (upper Hubbard band) with predominantly Cu 3d character, respectively. The strongest and most direct evidence for this comes from electron energy-loss spectroscopy (EELS)[4–7] and x-ray absorption spectroscopy (XAS).[8–11] In the case of p-type doping, the formation of holes on O sites can be directly measured while in the case of n-type doping a reduction of empty Cu 3d states is observed.

Although it is now generally believed that the states close to the Fermi energy E_F are mainly due to in-plane Cu and O orbitals, there is lively debate as to whether other orbitals such as Cu $3d_{3z^2-r^2}$, apical O $2p_z$, or in-plane O $2p_{x,y,z}$ (π bonded to Cu 3d) are important for transport properties and superconductivity in cuprates. An enhancement of T_c by the anharmonicity of vibra-

tions of apical oxygens has been proposed by Müller.[12] A model of high-T_c superconductivity based on d-d excitations was established by Weber.[13] Kamimura and Eto[14] have proposed that the mobile holes in p-type doped high-T_c superconductors are hybrids of Cu $3d_{3z^2-r^2}$ and apical O $2p_z$ orbitals. In their model, in the superconducting state, these mobile holes are paired due to the interaction with localized hybrids of Cu $3d_{x^2-y^2}$ and O $2p_\sigma$ orbitals. The importance of Cu $3d_{3z^2-r^2}$-O $2p_z$ hybrides and the formation of an "anti-Jahn-Teller" polaron was also stressed by Anisimov *et al.*[15] Their calculations predict an equal spectral weight of Cu $3d_{3z^2-r^2}$ states and O $2p_z$ states for the triplet spin polaron. On the other hand, other theories have predicted a suppression of superconductivity due to the influence of nonplanar orbitals. Maekawa and his co-workers[16] found a correlation between T_c and the energy difference between apical O $2p_z$ states and planar O $2p_\sigma$ states. From their analysis they concluded that in high-T_c compounds the Zhang-Rice singlet[17] formed of Cu $3d_{x^2-y^2}$ holes and O $2p_\sigma$ holes is stable. T_c is reduced due to a destabilization of the singlet by a mixing with apical O $2p_z$ states. Also Di Castro, Feiner, and Grilli[18] have explained the suppression of T_c above a certain dopant concentration by the occupancy of holes on Cu $3d_{3z^2-r^2}$-apical O $2p_z$ hybrids. The question whether a multiband approach is required has also been discussed by Eskes and Sawatzky.[19] Recently, Grant and McMahan have stressed the importance of apical O $2p_z$ states in determining the nature and the dispersion of quasiparticle states of p-type doped cuprates. From their limited-configuration-interaction calculations beyond Hartree Fock with an eight-band Hamiltonian for La_2CuO_4, they give detailed values for the number of hole states in Cu $3d_{x^2-y^2}$, Cu $3d_{3z^2-r^2}$, O $2p_\sigma$, and apical O $2p_z$ states for undoped and doped cuprates.[20]

Experimentally, most of the studies on the symmetry of hole states in cuprates have been performed on the $Bi_2Sr_2CaCu_2O_8$ system using XAS (Refs. 21–25) and EELS.[26] There is a general agreement among the various groups that holes on O have predominantly O $2p_{x,y}$ character. The number of holes in O $2p_z$ states with respect to the total number of holes on O sites is less than 2.5%. The holes on Cu sites have predominantly Cu $3d_{x^2-y^2}$ character. On the other hand, the number of Cu $3d_{3z^2-r^2}$ states and a possible energy shift between the $2p$-$3d_{x^2-y^2}$ and the $2p$-$3d_{3z^2-r^2}$ transition remain controversial. The ratio of the number of unoccupied Cu $3d_{3z^2-r^2}$ states with respect to the total number of unoccupied Cu $3d$ states varies between 4% and 20%. There have also been studies[26,27] on the symmetry of hole states in $YBa_2Cu_3O_7$ but in this case the problem is complicated due to the existence of CuO_3 chains.

In this contribution, we describe investigations on the symmetry of hole states on O and Cu sites in single crystals of $La_{2-x}Sr_xCuO_{4+\delta}$ (T phase) and $R_{2-x}Ce_xCuO_{4-\delta}$ (R =Nd, Sm) (T' phase) using XAS in the fluorescence-yield mode. Similar measurements on films of $La_{2-x}Sr_xCuO_{4+\delta}$ have been performed recently.[28] XAS in the fluorescence-yield mode is not surface sensitive in contrast to most of the other high-energy spectroscopies. In addition, it offers the possibility of measuring in a site-selective manner the local unoccupied density of states as well as the symmetry of the orbitals contributing to these states. In particular, when measuring O 1s and Cu 2p absorption edges in the cuprates, O 2p and Cu 3d states are probed, which predominantly determine the electronic structure of cuprates close to the Fermi level.

II. EXPERIMENT

Large single crystals (~5 mm×20 mm) of $La_{2-x}Sr_xCuO_{4+\delta}$ (x =0, 0.1, 0.15, 0.2, and 0.3) were grown by the traveling solvent floating-zone method using an NEC SC-15HD-II apparatus.[29] The inhomogeneity of the Sr concentration was less than ±0.01 for x =0.15 and 0.2 increasing to ±0.02 for x =0.3. For the $La_{1.9}Sr_{0.1}CuO_4$ single crystal, the estimated uncertainty in x was $0.09 \le x < 0.12$. The O content of all samples was close to 4. The undoped sample was annealed to remove excess O and to increase the Néel temperature. For x =0.1, 0.15, and 0.2, superconducting transition temperatures T_c =26.8, 35.7, and 32.6 K, respectively, were detected and a shielding signal of almost 100% was observed by means of dc susceptibility measurements. For x =0.3 superconductivity could not be detected for $T > 4.2$ K. Single crystals of $Nd_{2-x}Ce_xCuO_{4-\delta}$ (x =0.025, 0.15, and 0.22) were grown using a CuO-based flux method.[30] The crystals for x =0.15 showed a sharp transition at T_c =24 K after annealing in a reducing atmosphere. Single crystals of $Sm_{2-x}Ce_xCuO_{4-\delta}$ for x =0 and 0.15 were grown by a modified flux-flow method.[31] After the reduction process, the crystal with x =0.15 showed superconductivity below T_c =19.5 K. Meissner fractions of about 25% indicate that the crystals were bulk superconductors.

O 1s and Cu 2p absorption edges were recorded using synchrotron radiation from the *SX*700/II monochromator[32] operated by the Freie Universität Berlin at BESSY. The exit slit was set to 17 μm and the illumination of the ellipsoidal mirror was chosen to be 17%, yielding an instrumental energy resolution of $\Delta E \sim 740$ meV (full width at half maximum) at ~870 eV as derived by measuring the Ne 1s absorption line using a gas ionization cell. From the $\Delta E \propto E^{3/2}$ law, valid in the grazing-incidence range for a plane-grating monochromator, a resolution of ΔE =350 and 820 meV was estimated for the energies of the O 1s and Cu 2p absorption thresholds, respectively. The measurements of the $Nd_{2-x}Ce_xCuO_{4-\delta}$ and $Ca_{0.86}Sr_{0.14}CuO_2$ were performed with an energy resolution reduced by a factor of 1.5. The energy calibration was again performed by a measurement of the Ne 1s absorption line using the gas ionization cell. The intensity variation of the photon beam as a function of energy in the range of the O 1s absorption threshold was derived from total-electron-yield measurements of a clean Au surface. All O 1s absorption edges were corrected for this intensity variation. The XAS spectra were recorded via

the fluorescence-yield, using a windowless intrinsic Ge detector. The fluorescent x rays have a typical escape depth of 2000 Å. Therefore, this technique is not as surface sensitive as the partial electron-yield method where the escape depth is typically 50 Å. Compared to EELS in transmission with primary electron energies ≥ 100 keV, which is also not surface sensitive, the two yield methods in XAS have the advantage of much more straightforward sample preparation. For polarization-dependent EELS studies, single crystalline free-standing films are required, which are easy to prepare only in case of $Bi_2Sr_2CaCu_2O_8$.

For the fluorescence-yield studies the Ge detector was placed at an angle of 45° with respect to the incoming photon beam. The samples were mounted on a manipulator by which they could be rotated around the horizontal and vertical axes. In the case of $La_{2-x}Sr_xCuO_{4+\delta}$, large crystals were available allowing the preparation of **a**,*c* oriented slabs using an ultramicrotome with a diamond knife. The surface quality and the orientation were checked by polarization-dependent optical reflection spectroscopy,[33] which has roughly the same sampling depth as XAS in the fluorescence-yield mode. In order to perform orientation-dependent XAS measurements, the surface was oriented perpendicular to the incoming beam and the *a* or *c* axis was turned parallel to the **E** vector of the synchrotron radiation which lies in the horizontal plane. In the case of the $R_{2-x}Ce_xCuO_{4-\delta}$ crystals, only thin platelets with **a**,**b** surfaces were available. Therefore, spectra for $\mathbf{E}\perp c$ were taken with the *c*-axis parallel to the incoming photon beam. The sample was then rotated around the vertical axis by up to 85° in order to take spectra close to $\mathbf{E}\parallel c$.

Several experimental problems are encountered when monitoring small XAS signals parallel to the *c* axis in the presence of a large XAS signal parallel to the *a*,*b* plane. First, due to the finite vertical entrance aperture of the monochromator and due to a possible misalignment of the monochromator relative to the plane of the electron storage ring, the **E** vector of the synchrotron radiation has a small vertical component $\mathbf{E}_v$ in addition to the predominant horizontal component $\mathbf{E}_h$. A linear polarization $P=|\mathbf{E}_h|^2/(|\mathbf{E}_h|^2+|\mathbf{E}_v|^2)=97\pm1\%$ was estimated for the experimental configuration used. Second, the alignment of small crystals relative to the $\mathbf{E}_h$ vector of the synchrotron radiation is difficult to achieve. An alignment error of $\pm5°$ has been assumed. This value and the nonperfect polarization contribute to the error bars of the intensity ratio between states in orbitals parallel to the *c* axis to those perpendicular to the *c* axis. Further uncertainties may arise from misaligned grains or from polycrystalline or CuO_2-flux inclusions in the single crystals.

For XAS recorded in the transmission mode or in the electron-yield mode, as well as for EELS in transmission, it is well established that the measured absorption spectra are proportional to the absorption coefficient $\mu_A(E)$ of the absorbing element. In the case of the fluorescence detection the analysis of the measured spectra can be more complicated. The incoming photon intensity is attenuated by the total absorption coefficient, $\mu_T(E)$, resulting from all elements in the sample. When the core hole created by the absorption process at the atom of interest decays radiatively, the resulting fluorescence x-ray emission is proportional to the absorption cross section $\mu_A(E)$. The fluorescence x rays are then attenuated on their way to the surface by the total absorption coefficient $\mu_T(E_R)$ at the energy of the fluorescent radiation, E_R. In the case of almost completely filled valence shells, such as those of O^{2-} or Cu^{2+}, E_R is below the absorption threshold for the majority of the fluorescence radiation. A simple calculation shows that the intensity of the emitted fluorescence radiation, I_R, is then proportional to

$$I_R \propto I_0 f \frac{\mu_A(E)}{\mu_T(E)/\cos\alpha+\mu_T(E_R)/\cos\beta} , \tag{1}$$

where I_0 is the primary intensity, f is the fluorescence yield, α is the angle between the incoming beam and the surface normal, and β is the angle between surface normal and the outgoing beam towards the detector. Only in the limit of $\mu_A(E)\ll\mu_T(E)$ is the intensity of the fluorescence radiation proportional to $\mu_A(E)$. This holds for the O 1*s* preedges in cuprates, where $\mu_T(E)$ is dominated by absorption due to Cu and *R* atoms. In the case of the Cu 2*p* absorption edges, $\mu_A(E)$ in the range of the 2*p*-3*d* excitonic line is of the same order of magnitude as the absorption due to *R* elements and therefore the spectra have to be corrected according to Eq. (1). The absorption coefficients were taken from standard tables.[34,35] In the case of CuO near the 2*p*-3*d* excitonic line, $\mu_A(E)$ is close to $\mu_T(E)$ and much higher than $\mu_T(E_R)$. According to Eq. (1), the energy variation of the fluorescence yield is therefore strongly suppressed, requiring large corrections.

Using Fermi's "golden rule" the transition matrix elements relevant in this work with initial *s* and *p* states and linear polarization photons with the polarization vector in the direction $\mathbf{n}=(\sin\theta\cos\Phi,\sin\theta\sin\Phi,\cos\theta)$ can be calculated:[36]

$$\langle n_i s|H'|n_f p_x\rangle = -\overline{M}_{if}\sin\theta\cos\Phi , \tag{2a}$$

$$\langle n_i s|H'|n_f p_y\rangle = -\overline{M}_{if}\sin\theta\sin\Phi , \tag{2b}$$

$$\langle n_i s|H'|n_f p_z\rangle = -\overline{M}_{if}\cos\theta , \tag{2c}$$

$$\langle n_i p_x|H'|n_f d_{x^2-y^2}\rangle = \tfrac{1}{2}\sqrt{2}\,\overline{M}_{if}\sin\theta\cos\Phi , \tag{2d}$$

$$\langle n_i p_x|H'|n_f d_{3z^2-r^2}\rangle = \tfrac{1}{6}\sqrt{6}\,\overline{M}_{if}\sin\theta\cos\Phi , \tag{2e}$$

$$\langle n_i p_y|H'|n_f d_{x^2-y^2}\rangle = \tfrac{1}{2}\sqrt{2}\,\overline{M}_{if}\sin\theta\sin\Phi , \tag{2f}$$

$$\langle n_i p_y|H'|n_f d_{3z^2-r^2}\rangle = \tfrac{1}{6}\sqrt{6}\,\overline{M}_{if}\sin\theta\sin\Phi , \tag{2g}$$

$$\langle n_i p_z|H'|n_f d_{3z^2-r^2}\rangle = -\tfrac{1}{3}\sqrt{6}\,\overline{M}_{if}\cos\theta . \tag{2h}$$

H' is the Hamiltonian describing the electron-photon interaction, n_i and n_f are the principal quantum numbers of the initial and the final state, respectively, and $\overline{M}_{if}$ is determined by the reduced matrix elements. From the matrix elements given in Eqs. (2) the contributions of O $2p_{x,y,z}$ final states in O 1*s* absorption edges and of Cu $3d_{x^2-y^2}$ and Cu $3d_{3z^2-r^2}$ final states in Cu 2*p* absorption

edges can be calculated for a given polarization direction of photons relative to the crystal axis.

III. RESULTS

Polarization-dependent O 1s absorptions edges ($\mathbf{E}\perp c$ and $\mathbf{E}\|c$) for the antiferromagnetic insulator $La_2CuO_{4+\delta}$ and the p-type superconductor $La_{1.85}Sr_{0.15}CuO_{4+\delta}$ are shown in Figs. 1(a) and 1(b), respectively. Analogous data are presented in Figs. 2(a) and 2(b) for the antiferromagnetic insulator $Nd_{1.975}Ce_{0.025}CuO_{4-\delta}$ and the n-type doped superconductor $Nd_{1.85}Ce_{0.15}CuO_{4-\delta}$. Furthermore, we show in Fig. 3 analogous O 1s absorption edges for the insulating infinite layer system $Ca_{0.86}Sr_{0.14}CuO_2$, while Fig. 4 shows the O 1s absorption edges of $Nd_{1.975}Ce_{0.025}CuO_{4-\delta}$ as a function of the angle between vector $\mathbf{E}_h$ and the CuO_2 planes. All spectra presented in Figs. 1 to 4 are normalized in the energy range from 580 to 600 eV (not shown) and are not corrected for self-absorption. At such high energies, about 60 eV above Fermi level, the density of final states is believed to have almost free-electron character and should therefore be independent of doping concentration and orientation.

According to Eqs. (2), only s-p_z transitions are allowed

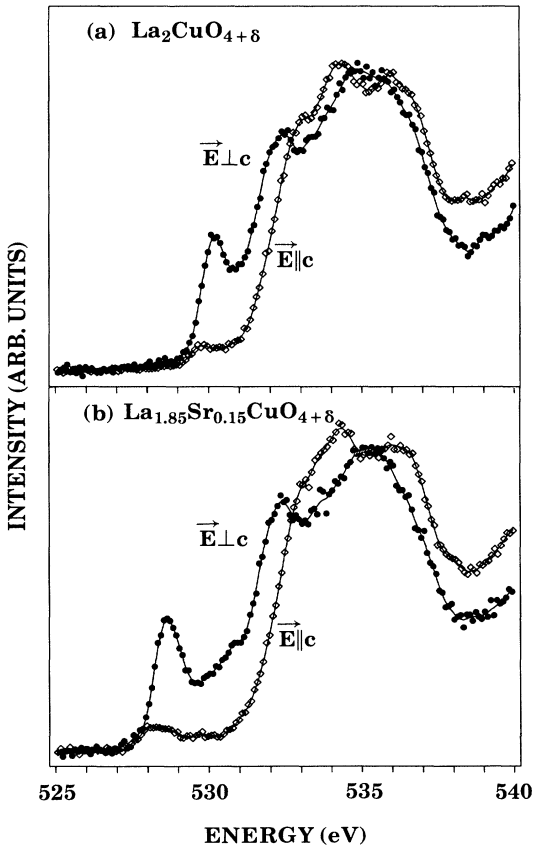

FIG. 1. Polarization-dependent O 1s x-ray absorption spectra of La cuprate single crystals: (a) insulating $La_2CuO_{4+\delta}$; (b) superconducting $La_{1.85}Sr_{0.15}Cu_{4+\delta}$. Closed circles: $\mathbf{E}\perp c$; open diamonds: $\mathbf{E}\|c$.

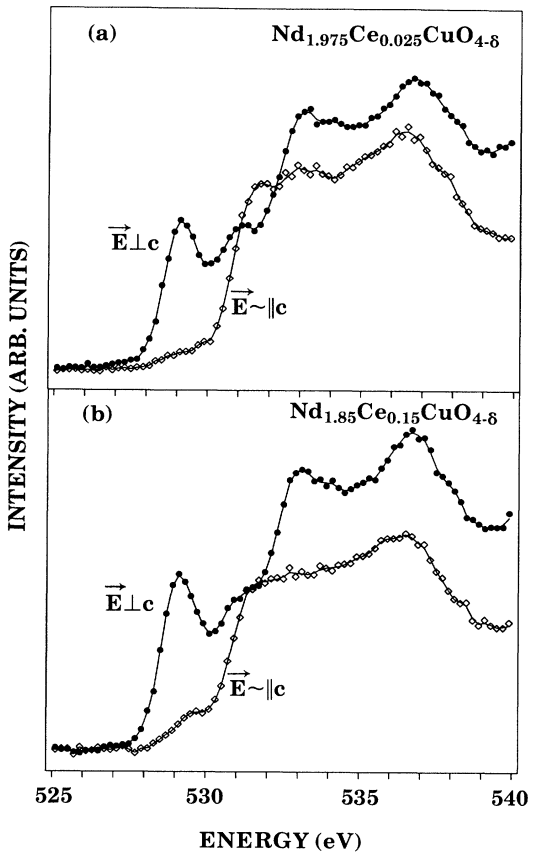

FIG. 2. Polarization-dependent O 1s x-ray absorption spectra of Nd cuprate single crystals: (a) insulating $Nd_{1.975}Ce_{0.025}CuO_{4-\delta}$; (b) superconducting $Nd_{1.85}Ce_{0.15}CuO_{4-\delta}$. Closed circles: $\mathbf{E}\perp c$; open diamonds: $\sphericalangle \mathbf{E},c = 5°$.

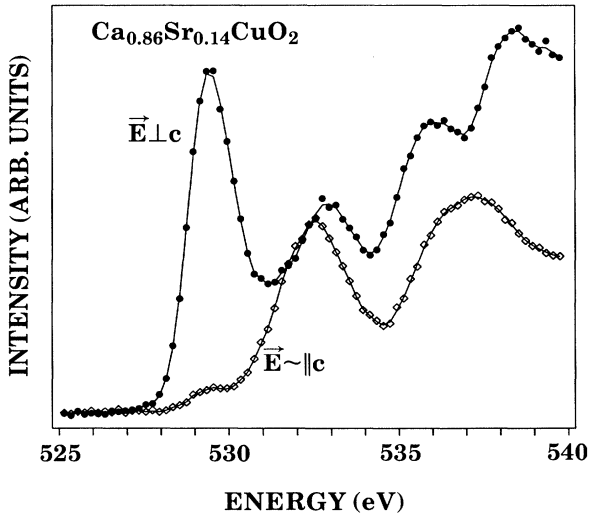

FIG. 3. Polarization-dependence O 1s x-ray absorption spectra of $Ca_{0.86}Sr_{0.14}CuO_2$. Closed circles: $\mathbf{E}\perp c$; open diamonds: $\sphericalangle \mathbf{E},c = 8°$.

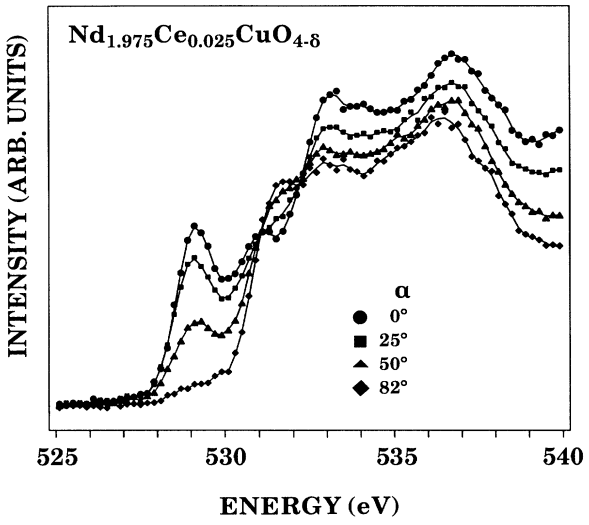

FIG. 4. Polarization-dependent O 1s x-ray absorption spectra of $Nd_{1.975}Ce_{0.025}CuO_{4-\delta}$ as a function of the angle, α, between the E vector of photons and the CuO_2 planes.

for $\mathbf{E}\|c$ ($\theta=0$) while for $\mathbf{E}\perp c$ ($\theta=90°$) s-p_x and s-p_y transitions are possible. In the latter case, for a square x,y plane, the transitions should be independent of ϕ ($\sin^2\phi+\cos^2\phi=1$) and only one half of the final states are seen in a given $\mathbf{E}\perp c$ spectrum. For example, for $\mathbf{E}\|a$, only unoccupied p_x states are observed but for a square x,y plane there are as many unoccupied p_y states.

For the $La_{2-x}Sr_xCuO_{4+\delta}$ system the spectral weight above 531.5 eV is almost independent of the doping concentration, x. As in previous investigations,[4-6,10] this spectral weight is therefore mainly attributed to the LaO planes, i.e., O 2p states hybridized with La 5d and 4f states or La 5d and 4f wave-function tails with p-like projection around O sites. Since the two LaO block layers per unit cell are also two-dimensional entities, they show considerable anisotropy between $\mathbf{E}\perp c$ and $\mathbf{E}\|c$. For $\mathbf{E}\perp c$, broad peaks at 532.4, 535, 541.5 (not shown), and 545 eV (not shown) are observed, while similar peaks appear for $\mathbf{E}\|c$ at 533, 534, 536, and 541 eV (not shown). The anisotropy decreases with increasing energy above threshold. Similarly, the spectral weight above 532 eV for the $R_{2-x}Ce_xCuO_{4-\delta}$ (R =Nd, Sm) systems is independent of x. This fact and the comparison with previous EELS measurements[7] of the O 1s absorption edge of Nd_2O_3 indicates that the intensity above 532 eV in the spectra shown in Figs. 2 and 4 is predominantly due to NdO planes, respectively. In $Nd_{2-x}Ce_xCuO_{4-\delta}$, for $\mathbf{E}\perp c$, broad peaks occur at ~531, 533, 537, 540, 543 (not shown), and 549 eV (not shown). For $\mathbf{E}\|c$, similar peaks are observed at ~532, 536.5, 542 (not shown), and 549 eV (not shown). Similar spectra are observed for $Sm_{2-x}Ce_xCu_{4-\delta}$ for $\mathbf{E}\perp c$ and $\mathbf{E}\|c$ (not shown). For $Ca_{0.86}Sr_{0.14}CuO_2$ the spectral weight above 531 eV can only be caused by O sites in the CuO_2 planes since the block layers formed by the Ca and Sr ions contain no O atoms. Therefore, this spectral weight is caused by O p states hybrized with Cu 3d, Cu 4s, Cu 4p, Ca 3d, and Sr 4d states.

In contrast to the higher-energy transitions, the preedge features in the O 1s absorption spectra for $La_{2-x}Sr_xCuO_{4+\delta}$ ($E<531.5$ eV) and $R_{2-x}Ce_xCuO_{4-\delta}$ (R =Nd,Sm) ($E<532$ eV) depend appreciably on dopant concentration and polarization. They do not appear in the O 1s absorption spectra of Nd_2O_3 and are therefore believed to originate from the CuO_2 planes. The preedge features are shown for the La system and for the Nd system in Figs. 5 and 6, respectively, as a function of doping concentration and for the polarization directions $\mathbf{E}\perp c$ and $E\|c$. For the undoped crystals ($x\simeq 0$) in both systems, the preedge features are almost identical. A peak at 530.2 eV for the La system and at 529.1 eV for the Nd system is observed. These peaks are assigned to transitions into the conduction band (upper Hubbard band) with predominantly Cu 3d character and an admixture of about 20% O 2p states. The energy difference between the preedge features of the La and the Nd systems agrees roughly with the one observed in previous unpolarized EELS studies.[7] It is due to both a reduced energy gap when going from the La system to the Nd system and to a chemical shift of the 1s level of O atoms in the CuO_2 plane.

In the La system, for $\mathbf{E}\perp c$, the preedge peak at 530 eV decreases in intensity and is shifted to higher energies with increasing x, in agreement with previous unpolarized EELS and XAS studies on polycrystalline samples.[6,10] A new peak, roughly proportional to x, appears at 528.5 eV upon doping. According to previous studies,[6,10] this low-energy prepeak is assigned to transitions

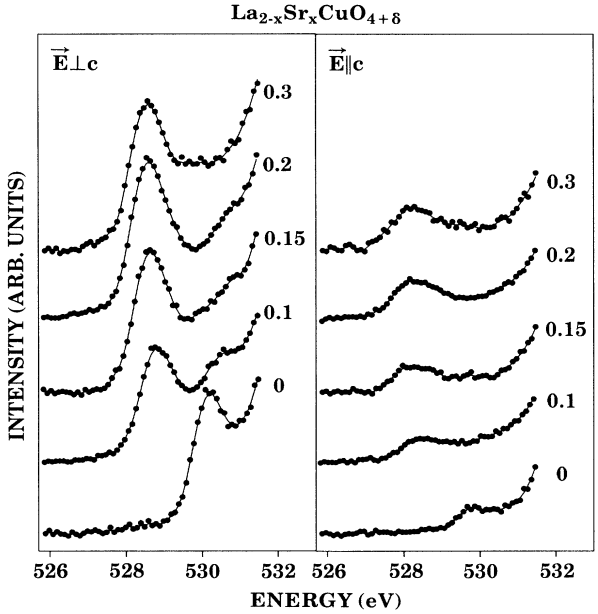

FIG. 5. Polarization and concentration-dependent O 1s x-ray absorption spectra in the preedge region of $La_{2-x}Sr_xCuO_{4+\delta}$ for $\mathbf{E}\perp c$ and $\mathbf{E}\|c$. The spectra are labeled by the concentration x.

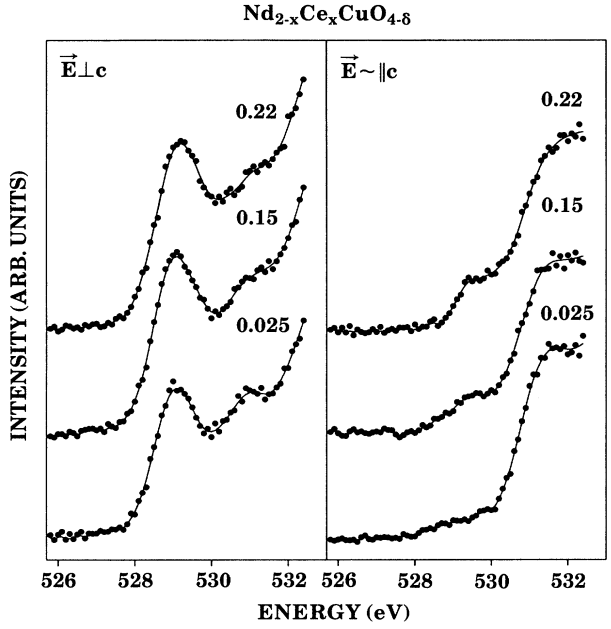

FIG. 6. Polarization- and concentration-dependent O 1s absorption edges in the preedge region of $Nd_{2-x}Ce_xCuO_{4-\delta}$ for $\mathbf{E}\perp c$ and $\sphericalangle \mathbf{E},c=8°$. The spectra are labeled by the concentration x.

into unoccupied O 2p states of the valence band. For $\mathbf{E}\|c$ the spectral weight of the preedge features is strongly reduced but shows a similar dependence on doping concentration. Furthermore, an energy shift of -0.3 eV is observed for the absorption edge, defined as the energy at half maximum, for doped samples of the La system between $\mathbf{E}\perp c$ and $\mathbf{E}\|c$. Since it is believed that these edges correspond to transitions into unoccupied O 2p states at the Fermi level, the observed shift can be explained in terms of a chemical shift of the O 1s level between in-plane O sites and apical O sites. This view is supported by LDA band-structure calculations[37] which predict that for La_2CuO_4 the binding energy of the 1s level for O sites in the LaO planes should be smaller than that for O sites in the CuO_2 planes. Therefore, the spectral weight of the valence-band peak for $\mathbf{E}\perp c$ is assigned to unoccupied O $2p_{x,y}$ states in the plane, while that for $\mathbf{E}\|c$ is assigned to unoccupied O $2p_z$ states from apical O sites. The same probably holds for the conduction-band states in the undoped samples, for which a chemical shift for the absorption thresholds of -0.3 eV is also observed between $\mathbf{E}\perp c$ and $\mathbf{E}\|c$. The intensity of the two prepeaks due to transitions into the valence band and to the conduction band as a function of x was determined by integrating the spectral weight of the difference between the $x=0$ spectrum and those with finite x up to 529.7 eV and between 529.7 and 530.7 eV. The results are shown in Fig. 7. In 7(a), the intensity of the valence band peak and that of the upper Hubbard band peak is plotted as a function of x for $\mathbf{E}\|c$ and $\mathbf{E}\perp c$. In addition, the fraction R of unoccupied O $2p_z$ states with respect to the total number of unoccupied O 2p states is shown in Fig. 7(b) for the valence band as a function of doping concentration x together with analogous data of Chen *et al.*[28] Note that in Ref. 28 intensity ratios between transitions into O $2p_z$ states to those into O $2p_x$ or O $2p_y$ states are given. Therefore, the fraction R given in the present investigation is about half as large as the ratio given in Ref. 28. For the conduction band, the fraction R is slightly above 10%, almost independent of the doping concentration, x. The numerical values for R are given in Table I.

In contrast to the preedge features for the p-type doped La system, those for the n-type doped Nd system exhibit no preedge features due to hole states in the valence band (see Fig. 6). This is in agreement with previous EELS (Refs. 7 and 38) and XAS (Refs. 39 and 40) studies. For $\mathbf{E}\perp c$ there is a slight increase of the intensity at 529 eV as a function of doping concentration. It is remarkable that in the spectra for $\mathbf{E}\perp c$, a peak at 531 eV is well pronounced in the undoped system and becomes progressively washed out at higher dopant concentrations. In previous EELS studies[38] of the Nd system it was realized that

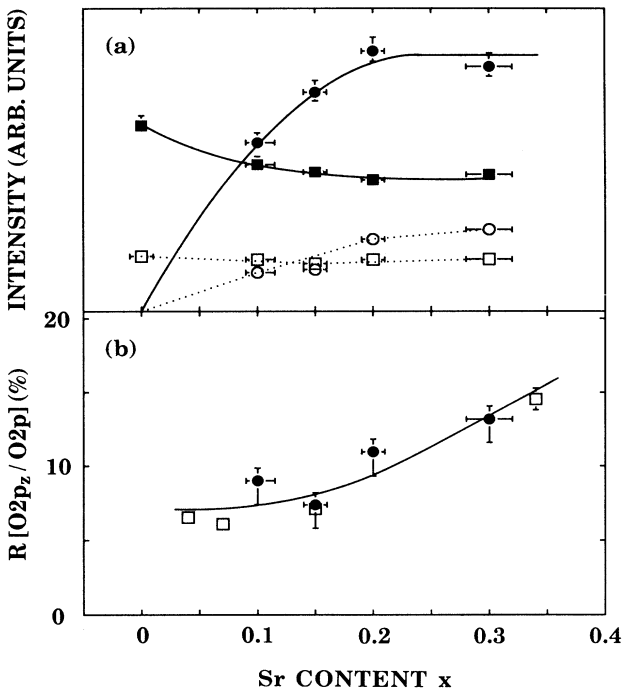

FIG. 7. (a) Intensity of hole states on O sites in $La_{2-x}Sr_xCuO_{4+\delta}$ as a function of Sr context x. Closed (open) circles: valence band, O $2p_{x,y}$ (O $2p_z$) symmetry. Closed (open) squares: upper Hubbard band, O $2p_{x,y}$ (O $2p_z$) symmetry. (b) Fraction R of unoccupied O $2p_z$ with respect to the total number of unoccupied O 2p states in the valence band of $La_{2-x}Sr_xCuO_{4-\delta}$. Closed circles: present investigation; open squares: data of Chen *et al.* (Ref. 28). Note that the values of Chen *et al.* are reduced by a factor of about 2, since in this present diagram the ratio of the number of holes on O $2p_z$ states to the total number of holes on O sites (O $2p_{x,y}$ and O $2p_z$) is plotted. The curves are guides to the eye.

TABLE I. Experimental fractions (in %) of holes in O $2p_z$ states with respect to the total number of O $2p$ hole states (columns 4 and 5) and holes in Cu $3d_{3z^2-r^2}$ states with respect to the total number of Cu $3d$ hole states (column 6) for $La_{2-x}Sr_xCuO_{4+\delta}$, $Nd_{2-x}Ce_xCuO_{4-\delta}$, and $Sm_{2-x}Ce_xCuO_{4-\delta}$, $\delta > 0$ annealed in argon, $\delta = 0$ as prepared. UHB, upper Hubbard band (defect states in this energy range may be included); VB, valence band; ga, $\mathbf{E}\|c$ measured at grazing angle; a,c, measured with $\mathbf{E}$ in the a,c plane.

			O $2p_z$/O $2p$		Cu $3d_{2z^2-r^2}$/Cu $3d$	
Sample	x	δ	UHB	VB	UHB	Geometry
$La_{2-x}Sr_xCuO_{4+\delta}$	0	0	12±1	· · ·	1±1	a,c
	0.1	0	14±1	9±1	3±1	a,c
	0.15	0	14±1	7±1	2±1	a,c
	0.2	0	15±1	11±1	3±1	a,c
	0.3	<0	15±2	13±1	5±1	a,c
$Sm_{2-x}Ce_xCuO_{4-\delta}$	0	0	6±1	· · ·	5±1	ga
	0	>0	11±1	· · ·	2±1	ga
	0.15	0	11±1	· · ·	3±1	ga
	0.15	>0	10±1	· · ·	5±1	ga
$Nd_{2-x}Ce_xCuO_{4-\delta}$	0.025	>0	4±1	· · ·	0±1	ga
	0.15	>0	6±1	· · ·	0±1	ga
	0.22	>0	8±1	· · ·	0±1	ga
$Ca_{0.86}Sr_{0.14}CuO_2$	0	· · ·	1±1	· · ·	2±1	ga

upon doping with Ce, additional spectral weight with strong O $2p_z$ character appears at ~530 eV. Since this was not observed in Th-doped samples, it was ascribed to Ce $5d$ and/or Ce $4f$ states hybridized with O $2p$ states. In the right-hand panel of Fig. 6, this spectral weight is clearly visible in the spectra recorded with $\mathbf{E}\sim\|c$. Its intensity increases with increasing x.

Since superconductivity appears in the n-type doped systems only after annealing in a reducing atmosphere, i.e., after O release, we have studied polarization-dependent preedge structures of as-grown and reduced crystals. Spectra of $Sm_{2-x}Ce_xCuO_{4-\delta}$ are shown for $x = 0$ and 0.15 and $\delta = 0$ and $\delta > 0$ in Fig. 8. Compared to the spectra of $Nd_{2-x}Ce_xCuO_{4-\delta}$ shown in Fig. 6, the data in Fig. 8 were taken with an improved energy resolution (see Sec. II). Once again, the spectral weight of O $2p_{x,y}$ states of the upper Hubbard band slightly increased upon doping for $\mathbf{E}\perp c$. Within error bars it does not change upon treatment in a reducing atmosphere. On the other hand, the peak at 531 eV is broadened not only upon doping but also upon O release. For $\mathbf{E}\sim\|c$ we clearly observed a peak at 529 eV for the undoped as-grown sample. From the fraction R of this peak for $\mathbf{E}\|c$ and $\mathbf{E}\perp c$ we conclude that about 10% of the O $2p$ states in the energy range of the conduction band have O $2p_z$ character, while the rest has O $2p_{x,y}$ character. For $\mathbf{E}\|c$ the peak at 529 eV seems to be only weakly influenced by doping and reducing; for $x = 0.15$ and/or $\delta > 0$, spectral weight appears at 529.5 eV. This indicates that similar unoccupied impurity states close to E_F with O $2p_z$ character are formed upon both doping with Ce and O release.

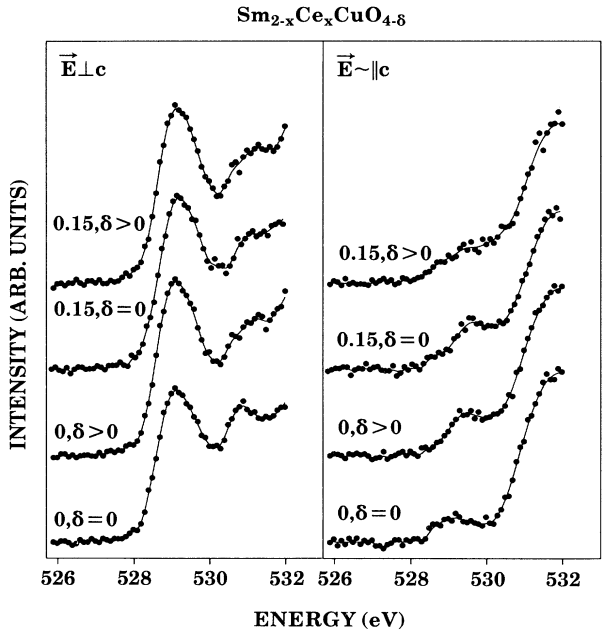

FIG. 8. Polarization-dependent O $1s$ x-ray absorption spectra in the preedge region of $Sm_2CuO_{4-\delta}$ and $Sm_{1.85}Ce_{0.15}CuO_{4-\delta}$. As-grown samples: $\delta = 0$; reduced samples: $\delta > 0$.

In Fig. 9(a) we show the intensity of unoccupied O $2p_{x,y}$ states and O $2p_z$ states in the range of the upper Hubbard band for $Nd_{2-x}Ce_xCuO_{4-\delta}$ and $Sm_{2-x}Ce_xCuO_{4-\delta}$. In Fig. 9(b) the fraction of O $2p_z$ holes with respect to the total number of holes on O sites is plotted as a function of x. Note that, not only O $2p$ states of the upper Hubbard band but also defect states due to Ce ions or due to O defects contribute to the observed O $2p_{x,y}$ and O $2p_z$ states.

In Fig. 10 we show Cu $2p_{3/2}$ absorption edges of insulating $La_2CuO_{4+\delta}$ and superconducting $La_{1.85}Sr_{0.15}CuO_{4+\delta}$ for $\mathbf{E}\perp c$ and $\mathbf{E}\|c$. Similar data are presented in Fig. 11 for insulating, as-prepared

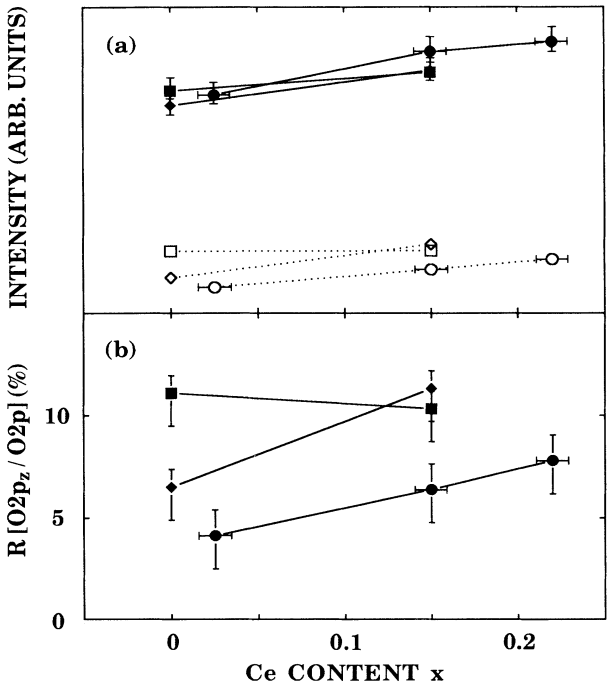

FIG. 9. Dependence on the Ce content x of (a) intensity of hole states on O sites contributing to the upper Hubbard band or O $2p$ states in the same energy range due to defect states related to dopant ions. Circles: $Nd_{2-x}Ce_xCuO_{4-\delta}$ ($\delta>0$, annealed in a reducing atmosphere); diamonds: $Sm_{2-x}Ce_xCuO_{4-\delta}$ ($\delta=0$, as prepared); squares: $Sm_{2-x}Ce_xCuO_{4-\delta}$ ($\delta>0$). (a) Closed symbols: O $2p_{x,y}$ states; open symbols: O $2p_z$ states. (b) Fraction R of unoccupied O $2p_z$ states relative to the total number of unoccupied O $2p$ states. The curves are guides to the eye.

$Sm_2CuO_{4-\delta}$ and superconducting $Sm_{1.85}Ce_{0.15}CuO_{4-\delta}$. Finally, we show in Fig. 12 polarization-dependent Cu $2p_{3/2}$ absorption edges for $Ca_{0.86}Sr_{0.14}CuO_2$. All the spectra in Figs. 10, 11, and 12 are normalized in the energy range close to 1000 eV and are not corrected for self-absorption. After that corrections the intensities of the first peak in the E$\perp c$ spectra will increase by a factor of 1.3 for the La and the Sm system. Due to a different experimental geometry, for $Ca_{0.86}Sr_{0.14}CuO_2$ the corrections are considerably smaller.

According to Eqs. (2), for E$\perp c$ ($\theta=90°$), transitions into unoccupied Cu $3d_{x^2-y^2}$ states and Cu $3d_{3z^2-r^2}$ can be observed, in the Cu $2p$ absorption edges assuming that other orbitals such as Cu $3d_{x,y}$ states, for example, are almost completely occupied because they are lower in energy. The square of the transition matrix element is three times larger for $3d_{x^2-y^2}$ orbitals than that for $3d_{3z^2-r^2}$ orbitals. Using Eqs. (2) and the same assumptions, for E$\|c$ only transitions into Cu $3d_{3z^2-r^2}$ states are possible. Thus, transitions into Cu $3d_{x^2-y^2}$ states and Cu $3d_{3z^2-r^2}$ can be separated from the two spectra. In all spectra for E$\perp c$ a pronounced peak at about 931 eV is observed. Since this peak is rather small for E$\|c$, where only Cu $3d_{3z^2-r^2}$ states are probed, a large fraction of the peak for E$\perp c$ can be attributed to transitions into in-plane Cu $3d_{x^2-y^2}$ states, indicating that most of the Cu $3d$ holes, independent of x, have $3d_{x^2-y^2}$ character. This is in agreement with several previous investigations.[24–26] Since the Cu $2p$-$3d$ transitions have strong excitonic character due to the interaction of $3d$ states with the $2p$ core hole, detailed information on the density of unoccupied $3d$ states cannot be derived from Cu $2p$ absorption edges. Nevertheless, the intensity in this excitonic line will be proportional to the number of $3d$ holes close to the Fermi level (i.e., in the upper Hubbard band). After background subtraction these intensities have been evaluated as a function of the dopant concentration for the La, Nd, and Sm systems as well as for $Ca_{0.86}Sr_{0.14}CuO_2$ for the two polarization directions. The number of holes close to E_F on Cu sites with $3d_{x^2-y^2}$ and $3d_{3z^2-r^2}$ symmetry, as derived from the intensity of the excitonic line, is shown in Fig. 13(a) for the La system. In addition, the fraction R of $3d_{3z^2-r^2}$ hole states with respect to the total number of Cu $3d$ hole states is shown in Fig. 13(b), together with similar data from Chen *et al.*[28] Analogous data for the $R_{2-x}Ce_xCuO_{4-\delta}$ (R =Nd and Sm) series of compounds are displayed in Figs. 14(a) and 14(b). The numerical

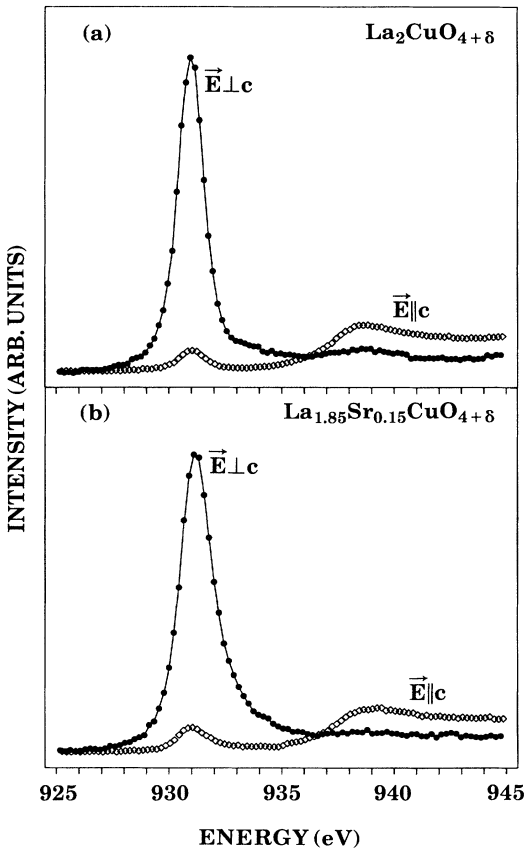

FIG. 10. Polarization-dependent Cu $2p_{3/2}$ x-ray absorption spectra of La cuprate single crystals: (a) insulating $La_2CuO_{4+\delta}$; (b) superconducting $La_{1.85}Sr_{0.15}CuO_{4+\delta}$. Closed circles: E$\perp c$; open diamonds: E$\|c$.

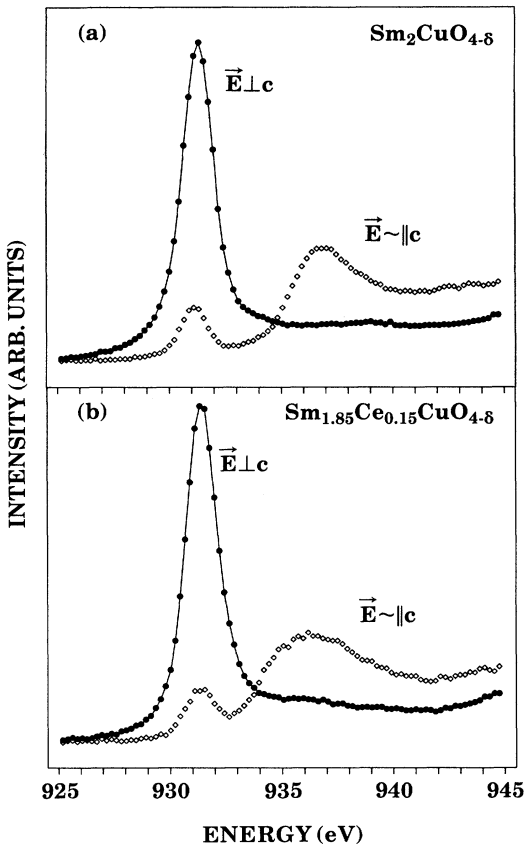

FIG. 11. Polarization-dependent Cu $2p_{3/2}$ x-ray absorption spectra of Sm cuprate single crystals: (a) insulating, as-prepared $Sm_2CuO_{4-\delta}$; (b) superconducting $Sm_{1.85}Ce_{0.15}CuO_{4-\delta}$. Closed circles: $\mathbf{E}\perp c$; open diamonds: $\sphericalangle \mathbf{E},c = 4°$.

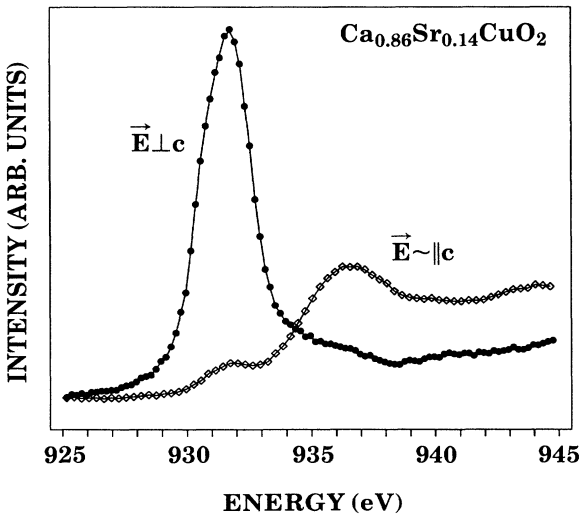

FIG. 12. Polarization-dependent Cu $2p_{3/2}$ x-ray absorption spectra of $Ca_{0.86}Sr_{0.14}CuO_2$ single crystals. Closed circles: $\mathbf{E}\perp c$; open diamonds: $\sphericalangle \mathbf{E},c = 5°$.

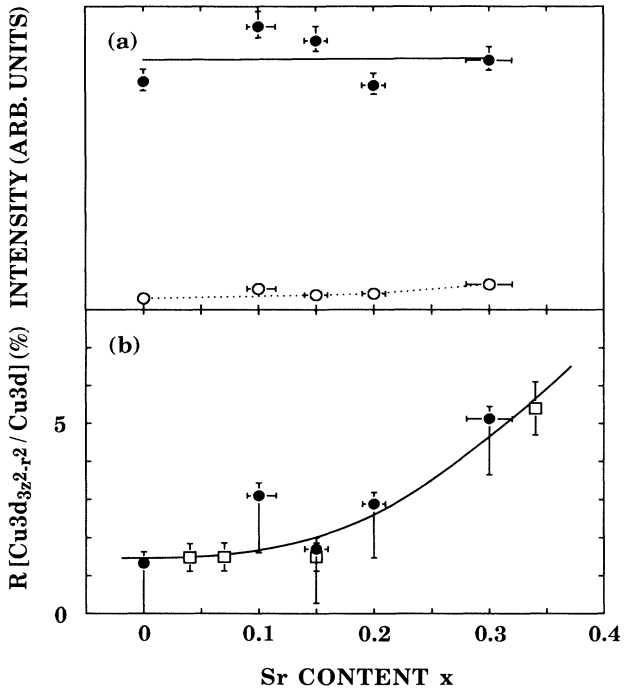

FIG. 13. Dependence on Sr content x of the intensity of hole states on Cu sites contributing to the excitonic line in $La_{2-x}Sr_xCuO_{4-\delta}$: (a) closed circles: Cu $3d_{x^2-y^2}$ states; open circles: Cu $3d_{3z^2-r^2}$ states. (b) Fraction R of unoccupied Cu $3d_{3z^2-r^2}$ states with respect to the total number of unoccupied Cu $3d$ states (near the Fermi level). Closed circles: present results; open squares: results from Chen *et al.* (Ref. 28). The curves are guides to the eye.

values of the fractions R of unoccupied Cu $3d_{3z^2-r^2}$ states in the excitonic line with respect to the total number of unoccupied Cu $3d$ states for all compounds studied in this work are given in Table I.

It is interesting to note the shape of the excitonic lines for $\mathbf{E}\perp c$. This line is quite symmetric for the undoped systems and remains so for the n-type doped system independent of the dopant concentration. However, for the p-type doped system, there is a clear asymmetry of the excitonic line due to a tail at the high-energy side. This additional spectral weight has already been explained in previous investigations in terms of holes on O sites shifting the Cu $2p$-$3d$ transition to higher energies.[41,42] The present study shows clearly that there are no holes on O sites in the n-type doped system.

There is considerable spectral weight for $\mathbf{E}\perp c$ and $\mathbf{E}\|c$ above the excitonic line extending at least up to 945 eV. Taking into account the matrix elements given in Eqs. (2) and subtracting the Cu $3d_{3z^2-r^2}$ contributions (derived from the $\mathbf{E}\|c$ spectra) from the $\mathbf{E}\perp c$ spectra, there is almost zero spectral weight between 935 and 945 eV in the $\mathbf{E}\perp c$ spectra. This means that all the spectral weight in Figs. 10, 11, and 12 above 935 eV originates from unoccupied Cu $3d_{3z^2-r^2}$ states. According to the dipole selection rule part of the spectral weight could also be due to transitions into unoccupied Cu $4s$ states. However, the

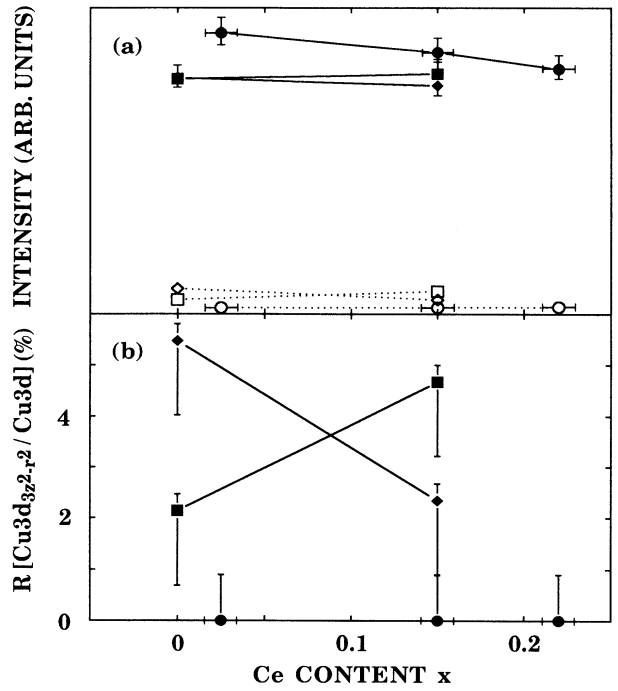

FIG. 14. Dependence on Ce context x of the intensity of hole states on Cu sites contributing the excitonic line in $Nd_{2-x}Ce_xCuO_{4-\delta}$ (circles), as prepared $Sm_{2-x}Ce_xCuO_{4-\delta}$ ($\delta=0$, diamonds), and annealed $Sm_{2-x}Ce_xCuO_{4-\delta}$ ($\delta=0$, squares). (a) Closed symbols: Cu $3d_{x^2-y^2}$ states; open symbols: Cu $3d_{3z^2-r^2}$ states. (b) Fraction R of unoccupied Cu $3d_{3z^2-r^2}$ states with respect to the total number of unoccupied Cu $3d$ states (near the Fermi level). The curves are guides to the eye.

matrix elements for $2p$-$4s$ transitions are about a factor of 30 smaller than those for $2p$-$3d$ transitions ruling out such an explanation. It is difficult to evaluate the amount of these unoccupied Cu $3d_{3z^2-r^2}$ states, since it is not clear how far up in energy these states extend. Furthermore, above ~950 eV the spectral weight due to Cu $2p_{3/2}$-$3d$ transitions is obscured by Cu $2p_{1/2}$-$3d$ transitions. A rough estimate gives that the amount of unoccupied Cu $3d_{3z^2-r^2}$ states in the energy range between 933 and ~945 eV is about 40% of the number of unoccupied Cu $3d$ states in the upper Hubbard band. The threshold for this spectral weight for $La_{2-x}Sr_xCuO_{4+\delta}$ is 937 eV, independent of x. For $Sm_{2-x}Ce_xCuO_{4-\delta}$, the threshold is at 935 eV for the undoped sample with $\delta=0$ and almost 1.5 eV lower for $x=0$ ($\delta>0$, reduced sample), $x=0.15$ ($\delta=0$), and $x=0.15$ ($\delta>0$, reduced sample) (see Fig. 11). The same shift is observed for the threshold between the undoped and metallic samples ($x=0.15$ and 0.22, $\delta>0$) of $Nd_{2-x}Ce_xCuO_{4-\delta}$.

IV. DISCUSSION

The present results support the general view that the hole states in the undoped parent compounds of cuprate superconductors and the extra holes formed upon p-type doping consist predominantly of in-plane orbitals in the CuO_2 plane, with Cu $3d_{x^2-y^2}$ and O $2p_{x,y}$ symmetry. The number of hole states in other orbitals, such as O $2p_z$ or Cu $3d_{3z^2-r^2}$, is about one order of magnitude lower. Additionally, band-structure calculations in the LDA have shown that the states near the Fermi level are dominated by Cu $3d_{x^2-y^2}$ orbitals strongly hybridized with O $2p_{x,y}$ orbitals.[43–46] The fact that the great majority of the hole states in cuprate superconductors are made up by in-plane orbitals explains why there is almost perfect agreement between the present data for $E\perp c$ and previous measurements on polycrystalline samples.[6,10]

To demonstrate this in detail, we first discuss the present O $1s$ absorption spectra of $La_{2-x}Sr_xCuO_{4+\delta}$ for $E\perp c$ and compare them with previous EELS and XAS measurements on polycrystalline samples.[6,10] The spectral weight for the addition of an electron to a CuO_2 plane (what is actually measured in XAS spectra neglecting core-hole effects) has been evaluated as a function of dopant concentration by cluster calculations in the framework of the three-band model.[47–49] A detailed calculation of O $1s$ absorption edges including the effects of core holes has been presented by Hybertsen *et al.*[50] In agreement with the experimental results, the calculations predict that the undoped compound is a charge transfer insulator with an upper Hubbard band composed of about 80% Cu $3d_{x^2-y^2}$ and 20% O $2p_{x,y}$ states. The latter can be seen in the O $1s$ absorption edges (see Fig. 5, $E\perp c$ and $x=0$). Upon doping, the Fermi level is pushed into the valence band, which has predominantly O $2p_{x,y}$ character. To be more explicit, there is an exchange interaction between the holes on O and holes on Cu sites, the latter already being present in the insulating parent compound. In this way singlet and triplet states are formed. The singlet states are split off from the valence band and upon doping, the Fermi level moves into these split-off states. This leads to the low-energy prepeak in Fig. 5, the intensity of which grows roughly in proportion to x (see Fig. 7). This does not hold for $x=0.3$, probably as in this case some of the hole states are filled due to an O deficiency ($\delta<0$). The threshold of the preedge for $x>0$ is shifted to lower energies since with increasing x, the Fermi level is pushed more and more into the valence band or rather into the split-off states of the valence band. A key signature of the correlated band situation together with strong covalency between Cu $3d$ and O $2p$ states is the observed transfer of oscillator strength from the second prepeak to the first prepeak for $x>0$, clearly seen in Fig. 5. In a one-band Hubbard picture without hopping, starting from the insulating half-filled case, upon forming a hole in the lower Hubbard band the upper Hubbard band loses one state while the lower gains two unoccupied states.[51] The fluctuations introduced by hopping lead to an additional dynamic transfer of oscillator strength which further enhances the strength of the low-energy peak at the expense of the higher-energy peak.[50] The situation is quite different from the uncorrelated insulator, where in a first approximation, the spectral weight of the conduction band would be unchanged and the number of holes in the valence band would be

proportional to x. Finally, we also mention that the shift of the conduction band to higher energies is explained by the calculation of Ref. 50.

In summary, the spectra for $\mathbf{E}\perp c$ as a function of x can be quantitatively explained in terms of a three-band Hubbard model using parameters derived from quantum-chemical calculations and which also fit other experimental data such as resonant photoemission measurements of cuprates.[52] Within this model, the Cu $2p_{3/2}$ absorption edge for $\mathbf{E}\perp c$ (see Fig. 10) can also be understood. The excitonic line is due to transitions into the upper Hubbard band having predominantly ($\sim 80\%$) Cu $3d_{x^2-y^2}$ orbital character. The intensity of this line is not changed substantially upon doping (see Fig. 13), since the excess holes are formed on O sites. Only the shape of the line is changed upon doping due to the influence of holes on O sites to the Cu $2p_{3/2}$-$3d$ transitions.

Now turning to the n-type doped Nd and Sm systems, the O $1s$ absorption edges for $\mathbf{E}\perp c$ in the prepeak region (see Figs. 6 and 8) are again very similar to spectra measured by EELS and XAS on polycrystalline samples.[7,38,39] The slight increase with increasing dopant concentration may be explained by defect states in the same energy range, having also O $2p_{x,y}$ character. The number of O $2p$ states hybridized to the upper Hubbard band does probably not change.

While discussing the prepeak of the O $1s$ absorption edges of $Nd_{2-x}Ce_xCuO_{4-\delta}$, we should explain the second peak in Fig. 6 for $\mathbf{E}\perp c$. According to the calculations of Ref. 50 it is due to the upper edge of the conduction band. In the La system, the spectral weight due to rare-earth $4f$ and $5d$ states is much closer to the upper Hubbard band than in the Nd system, and so the second peak is not visible in Fig. 5. Due to excitonic effects this peak is probably more pronounced in the insulating compound than in the metallic compounds.

Finally, we mentioned that in the Cu $2p_{3/2}$ edges of the Nd system, the intensity of the excitonic lines due to Cu $2p_{3/2}$-$3d_{x^2-y^2}$ transitions decreases with increasing dopant concentration (see Fig. 14), indicating a filling of Cu $3d$ states upon n-type doping. This is in agreement with previous EELS and XAS measurements on polycrystalline samples.[7,11] This result on the Cu states together with the fact that unoccupied O $2p$ states in the upper Hubbard band are not changed has been explained in terms of an n-type doped charge-transfer insulator.[7,11,38] The decrease of unoccupied Cu $3d$ states upon n-type doping is not observed for the Sm system. The reason for this is not clear at present.

In the following we discuss hole states in nonplanar orbitals. For the undoped La system about 12% of the total amount of O $2p$ states hybridized to the upper Hubbard band have p_z character. As mentioned before, the spectral weight of these O $2p_z$ holes is probably caused by the apical-O sites. Band-structure calculations in the LDA approximation for La_2CuO_4 predict that 8% of the total amount of O $2p$ states (predominantly in in-plane O $2p_\sigma$ states) are in apical O $2p_z$ states,[53] in fair agreement with the present experimental results. However, we note that the limited configuration interaction calculations beyond Hartree Fock for an eight-band effective Hamiltonian for La_2CuO_4 by Grant and McMahan[20] give no evidence for any significant O $2p_z$ hole states. Nevertheless, the error bars for the experimental ratios of O $2p_z$ to O $2p$ hole states is about 1%, i.e., much smaller than the value of 12%. In addition, Chen *et al.*[28] reported a similar value. Thus, the experimental results clearly indicate the admixture of a considerable amount of O $2p_z$ states to the upper Hubbard band. In Nd_2CuO_4 and Sm_2CuO_4 the amount of O $2p_z$ states hybridized to the upper Hubbard band is 3 (extrapolated to $x=0$) and 6%, respectively, of the total number of unoccupied O $2p$ states. These high numbers, in particular for Sm_2CuO_4, are difficult to understand since in these compounds there are no apical O sites. The distance of the O sites in the NdO planes to the Cu sites is much larger than the apical-O to Cu distance in La_2CuO_4. Therefore, the hybridization of O $2p_z$ states from O sites in NdO or SmO planes to the upper Hubbard band is very unlikely. The spectral weight of the prepeak for $\mathbf{E}\|c$ may then be explained by O $2p_z$ states from the CuO planes. This is supported by the fact that in Sm_2CuO_4 no chemical shift between the prepeaks for $\mathbf{E}\perp c$ and $\mathbf{E}\|c$ is observed. To our knowledge, there exist no band-structure calculations on the T' phase which give detailed numbers on the orbital- and site-selective character of unoccupied O $2p$ states.

The extra holes formed in the valence band upon p-type doping the La system have predominantly O $2p$ character. For $x \leq 0.15$, about 8% have O $2p_z$ character (distributed over the two apical O sites per unit cell), the majority originating from in-plane O $2p_{x,y}$ states. For $x=0.3$, a fraction of 13% of O $2p_z$ states has been determined. These values are in excellent agreement with those reported by Chen *et al.*[28] The present value of about 8% for $x \leq 0.15$ (low doping concentration) agrees perfectly with the value of 8% calculated by Grant and McMahan[20] for the single hole-doped insulator using an eight-band Hamiltonian. It is interesting to note, however, that LDA band-structure calculations[57] predict 25% of the additional unoccupied O $2p$ states, formed upon Sr doping with $x=0.15$, to have apical O $2p_z$ character, in clear disagreement with the experimental results.

For the n-type doped cuprates, the O $2p_z$ fraction in the upper Hubbard band remains constant with doping. However, additional O $2p_z$ states appear upon doping, at about 0.5 eV higher energies leading to an increase of the observed intensity in this energy range for $\mathbf{E}\sim\|c$. These have been previously ascribed to Ce $5d$ and Ce $4f$ hybridized to O $2p$ states.[7] In band-structure calculations, using a supercell, Ce $5d$ states have been predicted[54] close to the Fermi level. This additional spectral weight appearing upon Ce doping has also been observed in EELS measurements on both polycrystalline and single-crystalline samples.[38] The assignment of the extra O $2p_z$ states to Ce-induced impurity states is supported by the fact that these states are not observed in Th-doped Nd_2CuO_4.[38] It is interesting to note that similar impurity states appear at the same energy upon annealing in a reducing atmosphere, i.e., by O release. There is almost no change of this spectral weight when a Ce doped sample is

reduced. Treatment of a doped sample in a reducing atmosphere is essential for the appearance of superconductivity. The present measurements do not give a clear indication of a significant change of the electronic structure at the Fermi level of doped samples during the annealing process. More systematic measurements are necessary to solve this problem.

The fractions R of unoccupied Cu $3d_{3z^2-r^2}$ states in the energy range of the excitonic line with respect to the total number of unoccupied Cu $3d$ states given in Table I and in Figs. 13 and 14, are $3\pm3\%$. In the Sm systems these values are considerably larger. The reason for this is not clear. The present results for the La system agree with the data of Chen *et al.*,[28] which gave a smaller value of R for low dopant concentrations. The larger R value for $x=0.3$ supports the simple picture that due to the increasing number of holes on O sites in the CuO_2 plane, the crystal field at the Cu sites changes in such a way as to lower Cu $3d_{x^2-y^2}$ states and raise the Cu $3d_{3z^2-r^2}$ states.[55] This leads to an increasing number of holes on Cu $3d_{3z^2-r^2}$ orbitals with increasing dopant concentration. On the other hand, the weak Cu $3d_{3z^2-r^2}$ character of the upper Hubbard band is in agreement with the calculations of Grant and McMahan,[20] which give $R=0.3\%$ and $R=1.9\%$ for the undoped and the hole-doped compounds, respectively. LDA band-structure calculations[53] on $La_{2-x}Sr_xCuO_4$ predict $\sim4\%$ ($x=0$) and 5% ($x=0.15$) of the unoccupied Cu $3d$ states to have Cu $3d_{3z^2-r^2}$ character. To our knowledge, no detailed numbers for the T'-phase compounds are available.

The well-pronounced edges in the Cu $2p_{3/2}$ absorption spectra several eV above the excitonic line have predominantly Cu $3d_{3z^2-r^2}$ character. According to Grioni *et al.*,[56] these states may be strongly hybridized with Cu $4s$ states. Mei and Stollhoff[57] have performed *ab initio* calculations on the charge distribution and orbital character of these states in (Cu_mO_n) clusters. Without taking into account Cu $4s,4p$ orbitals, the number of unoccupied Cu $3d_{3z^2-r^2}$ states was found to be negligible. However, the addition of Cu $4s$ and Cu $4p$ orbitals induced a reduction of the filling of Cu $3d_{3z^2-r^2}$ states due to hybridization with the former orbitals. Then, about 20% of the total number of holes on Cu sites have $3d_{3z^2-r^2}$ character. Probably, a large fraction of the spectral weight in the Cu $2p$ edges between 933 and 940 eV is due to these Cu $3d_{3z^2-r^2}$ states hybridized with Cu $4s,4p$ states. On the other hand, a hybridization with other states, such as La $5d$, may also be possible. The shift towards the excitonic line upon reducing and/or doping in the Sm system (see Fig. 11) may indicate that the Cu $4s$ band or other states, such as Ce $5d$ or $4f$, may shift towards the Fermi level. The additional spectral weight observed in the O $1s$ absorption edges upon reducing and/or doping may be related to such a shift of electronic states towards the Fermi level.

The present results rule out theories for high-T_c superconductivity which are based on a large fraction of Cu $3d_{3z^2-r^2}$ holes close to the Fermi level. Such theories include, for example, the formation of mobile holes on p-type doped cuprates by Cu $3d_{3z^2-r^2}$ and apical O $2p_z$ hybrids.[14] In the model for high-T_c superconductivity based on d-d excitations,[13] unoccupied Cu $3d_{3z^2-r^2}$ states would enhance the oscillator strength of d-d transitions. Moreover the small number of unoccupied Cu $3d_{3z^2-r^2}$ states near the Fermi level does not support the formation of "anti-Jahn-Teller" polarons.

On the other hand, there are theories which claim that superconductivity is suppressed by holes on apical-O sites.[16,18] Although the present results do not provide a clear correlation between the number of O $2p_z$ holes and T_c, the fact that the number of these holes increases at high-dopant concentration ($x\sim0.3$) supports such theories. However, recent investigations of T_c as a function of x, indicate that superconductivity is suppressed at $x\sim0.25$ due to a phase transition from the orthorhombic to a tetragonal structure.[58] The fact that the number of O $2p_z$ states is considerably lower in $Bi_2Sr_2CaCu_2O_8$ ($T_c\sim80$ K) compared to $La_{1.85}Sr_{0.15}CuO_4$ ($T_c=35$ K) can also be taken as evidence that holes on apical O are detrimental to superconductivity. Further systematic studies on other systems are necessary to obtain a clear answer to the question as to whether holes on O $2p_z$ states influence superconductivity in cuprates. Certainly the increase of holes in apical O sites with increasing x can be related to the fact that metallic conductivity parallel to the c axis is observed at higher dopant concentrations.[59]

V. SUMMARY

Using polarization-dependent XAS measurements of O $1s$ and Cu $2p_{3/2}$ absorption edges on single crystals of cuprate high-T_c superconductors and their insulating parent compounds, the symmetry of states close to the Fermi level has been determined. It has been clearly shown that these states have predominantly in-plane O $2p_{x,y}$ and Cu $3d_{x^2-y^2}$ character.

About 12% of the total number of O $2p$ states hybridized with states of the upper Hubbard band of undoped La_2CuO_4 have O $2p_z$ character. For $x<0.2$ about 8% of the total number of holes on O sites formed upon p-type doping have O $2p_z$ character. In the p-type doped cuprates, these holes are probably formed on the apical O sites. The hole states on Cu close to the Fermi level, which are already present in the insulating parent compounds, have about 3% Cu $3d_{3z^2-r^2}$ character. Probably due to hybridization with Cu $4s$ and $4p$ states, there is a considerable amount of unoccupied Cu $3d_{3z^2-r^2}$ states several eV above the Fermi level. The experimental results on nonplanar contributions to hole states close to the Fermi level with the exception of O $2p_z$ states in the upper Hubbard band agree qualitatively with recent theoretical cluster calculations[20] based on an eight-band effective Hamiltonian.

ACKNOWLEDGMENT

Expert assistance by the staff of BESSY is acknowledged. The work in Berlin was supported by the Bundesministerium für Forschung und Technologie, Project No. 05-5KEAXT/TPOL.

[1]V. J. Emery, Phys. Rev. Lett. **58**, 2794 (1987).
[2]C. M. Varma, S. Schmitt-Rink, and E. Abrahams, Solid State Commun. **62**, 681 (1987).
[3]J. Zaanen, G. A. Sawatzky, and J. W. Allen, Phys. Rev. Lett. **55**, 418 (1985).
[4]N. Nücker, J. Fink, B. Renker, D. Ewert, C. Politis, P. J. W. Weijs, and J. C. Fuggle, Z. Phys. B **67**, 9 (1987).
[5]N. Nücker, J. Fink, J. C. Fuggle, P. J. Durham, and W. M. Temmerman, Phys. Rev. B **37**, 5158 (1988).
[6]H. Romberg, M. Alexander, N. Nücker, P. Adelmann, and J. Fink, Phys. Rev. B **42**, 8768 (1990).
[7]M. Alexander, H. Romberg, N. Nücker, P. Adelmann, J. Fink, J. T. Markert, M. B. Maple, S. Uchida, H. Takagi, Y. Tokura, A. C. W. P. James, and D. W. Murphy, Phys. Rev. B **43**, 333 (1991).
[8]J. A. Yarmoff, D. R. Clarke, W. Drube, U. O. Karlsson, A. Taleb-Ibrahimi, and F. J. Himpsel, Phys. Rev. B **36**, 3967 (1987).
[9]P. Kuiper, G. Kruizinga, J. Ghijsen, M. Grioni, P. J. W. Weijs, F. M. F. de Groot, G. A. Sawatzky, H. Verweij, L. F. Feiner, and H. Petersen, Phys. B **38**, 6483 (1988).
[10]C. T. Chen, F. Sette, Y. Ma, M. S. Hybertsen, E. B. Stechel, W. M. C. Foulkes, M. Schlüter, S.-W. Cheong, A. S. Cooper, L. W. Rupp, Jr., B. Batlogg, Y. L. Soo, Z. H. Ming, A. Krol, and Y. H. Kao, Phys. Rev. Lett. **66**, 104 (1991).
[11]C. F. J. Flipse, G. van der Laan, A. L. Johnson, and K. Kadowaki, Phys. Rev. B **42**, 1997 (1990).
[12]K. A. Müller, Z. Phys. B **80**, 193 (1990).
[13]W. Weber, Z. Phys. B **70**, 323 (1988).
[14]H. Kamimura and M. Eto, J. Phys. Soc. Jpn. **59**, 3053 (1990).
[15]V. I. Anisimov, M. A. Korotin, J. Zaanen, and O. K. Andersen, Phys. Rev. Lett. **68**, 345 (1992).
[16]Y. Ohta, T. Tohyama, and S. Maekawa, Phys. Rev. B **43**, 2968 (1991).
[17]F. C. Zhang and T. M. Rice, Phys. Rev. B **37**, 3759 (1988).
[18]C. Di Castro, L. F. Feiner, and M. Grilli, Phys. Rev. Lett. **66**, 3209 (1991).
[19]H. Eskes and G. A. Sawatzky, Phys. Rev. B **44**, 9656 (1991).
[20]J. B. Grant and A. K. McMahan, Phys. Rev. B **46**, 8440 (1992).
[21]F. J. Himpsel, G. V. Chandrashekhar, A. B. McLean, and M. W. Shafer, Phys. Rev. B **38**, 11 946 (1988).
[22]P. Kuiper, M. Grioni, G. A. Sawatzky, D. B. Mitzi, A. Kapitulnik, A. Santaniello, P. de Padova, and P. Thiry, Physica C **157**, 260 (1989).
[23]M. Abbate, M. Sacchi, J. J. Wnuk, L. W. M. Schreurs, Y. S. Wang, R. Lof, and J. C. Fuggle, Phys. Rev. B **42**, 7914 (1990).
[24]S. Suzuki, T. Takahashi, T. Kusunoki, T. Morikawa, S. Sato, H. Katayama-Yoshida, A. Yamanaka, F. Minami, and S. Takekawa, Phys. Rev. B **44**, 5381 (1991).
[25]A. Bianconi, S. Della Longa, C. Li, M. Pompa, A. Congiu-Castellano, D. Udron, A. M. Flank, and P. Lagarde, Phys. Rev. B **44**, 10 126 (1991).
[26]N. Nücker, H. Romberg, X. X. Xi, J. Fink, B. Gegenheimer, and Z. X. Zhao, Phys. Rev. B **39**, 6619 (1989).
[27]A. Krol, Z. H. Ming, Y. H. Kao, N. Nücker, G. Roth, J. Fink, G. C. Smith, K. T. Park, J. Yu, A. J. Freeman, A. Erb, G. Müller-Vogt, J. Karpinski, E. Kaldis, and K. Schönmann, Phys. Rev. B **45**, 2581 (1992).
[28]C. T. Chen, L. H. Tjeng, J. Kwo, H. L. Kao, P. Rudolf, F. Sette, and R. M. Fleming, Phys. Rev. Lett. **68**, 2543 (1992).
[29]K. Oka and H. Unoki, in *Advances in Superconductivity II,* edited by T. Ishiguro and K. Kajimura (Springer-Verlag, Tokyo, 1990), pp. 251–254.
[30]J. L. Peng, Z. Y. Li, and R. L. Greene, Physica C **177**, 79 (1991).
[31]J. Markl, J. P. Ströbel, M. Klauda, and G. Saemann-Ischenko, J. Cryst. Growth **113**, 395 (1991).
[32]M. Domke, T. Mandel, A. Puschmann, C. Xue, D. A. Shirley, G. Kaindl, H. Petersen, and P. Kuske, Rev. Sci. Instrum. **63**, 80 (1992).
[33]A. Zibold, K. Widder, H. P. Geserich, G. Bräuchle, H. Claus, H. von Löhneysen, N. Nücker, A. Erb, and G. Müller-Vogt (unpublished).
[34]W. J. Veigele, in *Handbook of Spectroscopy,* edited by J. W. Robinson (CRC Press, Cleveland, OH, 1974), Vol. 1, pp. 28–154.
[35]B. L. Henke and E. S. Ebisu, in *Advanced X-Ray Analysis,* edited by C. L. Grant *et al.* (Plenum, New York, 1973), Vol. 17, p. 150.
[36]See, e.g., D. D. Vvedensky, in *Unoccupied Electronic States,* edited by J. C. Fuggle and J. E Inglesfield (Springer, Berlin, 1992), pp. 139–176.
[37]J. Redinger, J. Yu, A. J. Freeman, and P. Weinberger, Phys. Lett. A **124**, 463 (1987).
[38]J. Fink, N. Nücker, M. Alexander, H. Romberg, M. Knupfer, M. Merkel, P. Adelmann, R. Claessen, G. Mante, T. Buslaps, S. Harm, R. Manzke, and M. Skibowski, Physica C **185–189** 45 (1991).
[39]A. Krol, C. S. Lin, Z. H. Ming, C. J. Sher, Y. H. Kao, C. L. Lin, S. L. Qiu, J. Chen, J. M. Tranquada, M. Strongin, G. C. Smith, Y. K. Tao, R. L. Meng, P. H. Hor, C. W. Chu, G. Cao, and J. E. Crow, Phys. Rev. B **42**, 4763 (1990).
[40]T. Takahashi, H. Katayama-Yoshida, and H. Matsuyama, Z. Phys. B **78**, 343 (1990).
[41]A. Bianconi, A. Congiu-Castellano, M. De Santis, P. Rudolf, P. Lagarde, A. M. Flank, and A. Marcelli, Solid State Commun. **63**, 1009 (1987).
[42]D. D. Sarma, O. Strebel, C. T. Simmons, U. Neukirch, G. Kaindl, R. Hoppe, and H. P. Müller, Phys. Rev. B **37**, 9784 (1988).
[43]L. F. Mattheiss, Phys. Rev. Lett. **58**, 1028 (1987).
[44]J. Yu, A. J. Freeman, and J.-H. Xu, Phys. Rev. Lett. **58**, 1035 (1987).
[45]W. E. Pickett, Rev. Mod. Phys. **61**, 433 (1989).
[46]S. Massidda, N. Hamada, J. Yu, and A. J. Freeman, Physica C **157**, 571 (1989).
[47]W. Stephan and P. Horsch, in *Dynamics of Magnetic Fluctuations in High Temperature Superconductors,* edited by G. Reiter, P. Horsch, and G. Psaltakis (Plenum, New York, 1990).
[48]T. Tohyama and S. Maekawa, Physica C **191**, 193 (1992).
[49]J. Wagner, W. Hanke, and D. J. Scalapino, Phys. Rev. B **43**, 10 517 (1991).
[50]M. S. Hybertsen, E. B. Stechel, W. M. C. Foulkes, and M. Schlüter, Phys. Rev. B **45**, 10 032 (1992).
[51]H. Eskes, M. B. J. Meinders, and G. A. Sawatzky, Phys. Rev. Lett. **67**, 1035 (1991).
[52]J. Ghijsen, L. H. Tjeng, J. van Elp, H. Eskes, J. Westerink, G. A. Sawatzky, and M. T. Czyzyk, Phys. Rev. B **38**, 11 322 (1988).
[53]J. Zaanen, O. Jepsen, O. Gunnarsson, A. T. Paxton, O. K. Andersen, and A. Svane, Physica C **153**, 1636 (1988); (private communication).
[54]G. Y. Guo, Z. Szotek, and W. M. Temmerman, Physica C **162**, 1351 (1989).

[55]D. I. Khomskii and E. I. Neimark, Physica C **173**, 342 (1991).
[56]M Grioni, J. B. Goedkoop, R. Schoorl, F. M. F. de Groot, J. C. Fuggle, F. Schäfers, E. E. Koch, G. Rossi, J.-M. Esteva, and R. C. Karnatak, Phys. Rev. B **39**, 1541 (1989).
[57]C.-J. Mei and G. Stollhoff, Phys. Rev. B **43**, 3065 (1991).
[58]H. Takagi, R. J. Cava, M. Marezio, B. Batlogg, J. J. Krajewski, W. F. Peck, Jr., P. Bordet, and D. E. Cox, Phys. Rev. Lett. **68**, 3777 (1992).
[59]T. Ito, Y. Nakamura, H. Takagi, and S. Uchida, Physica C **185–189**, 1267 (1991).